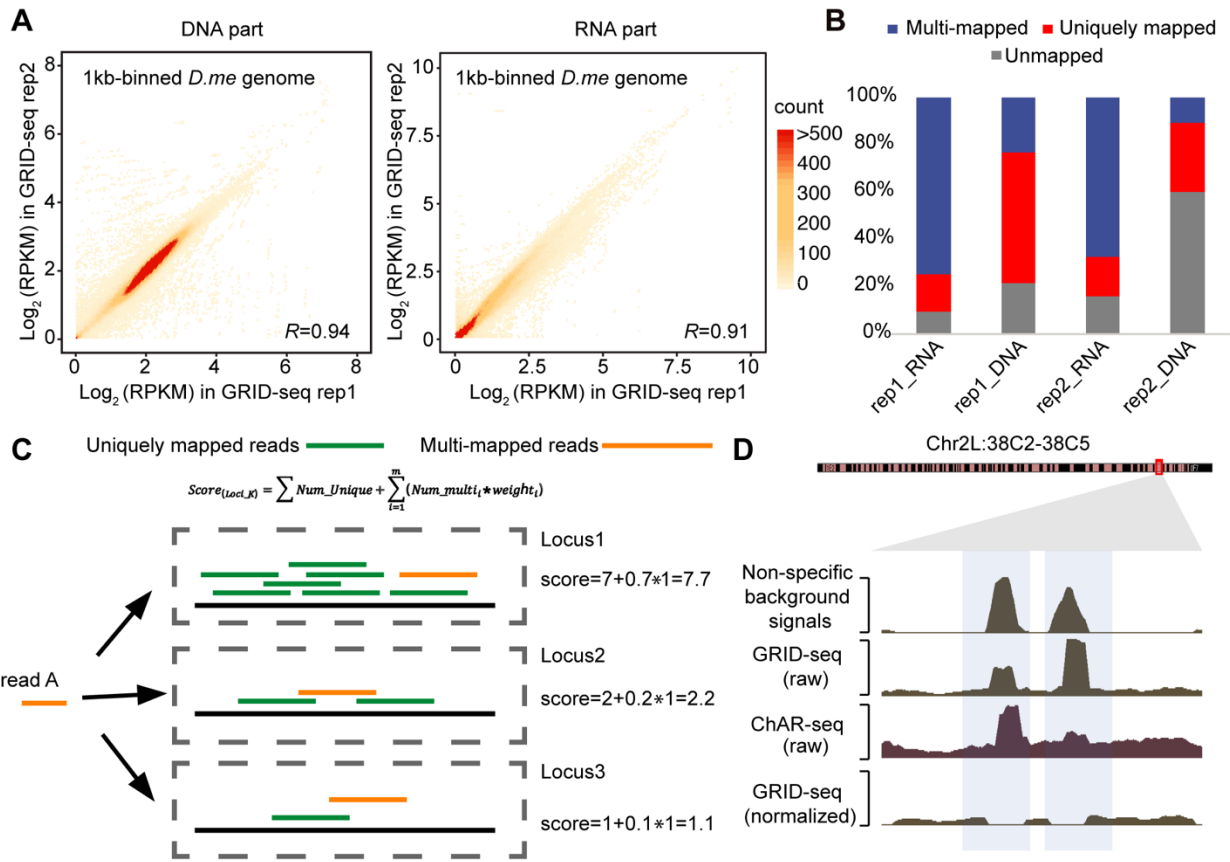


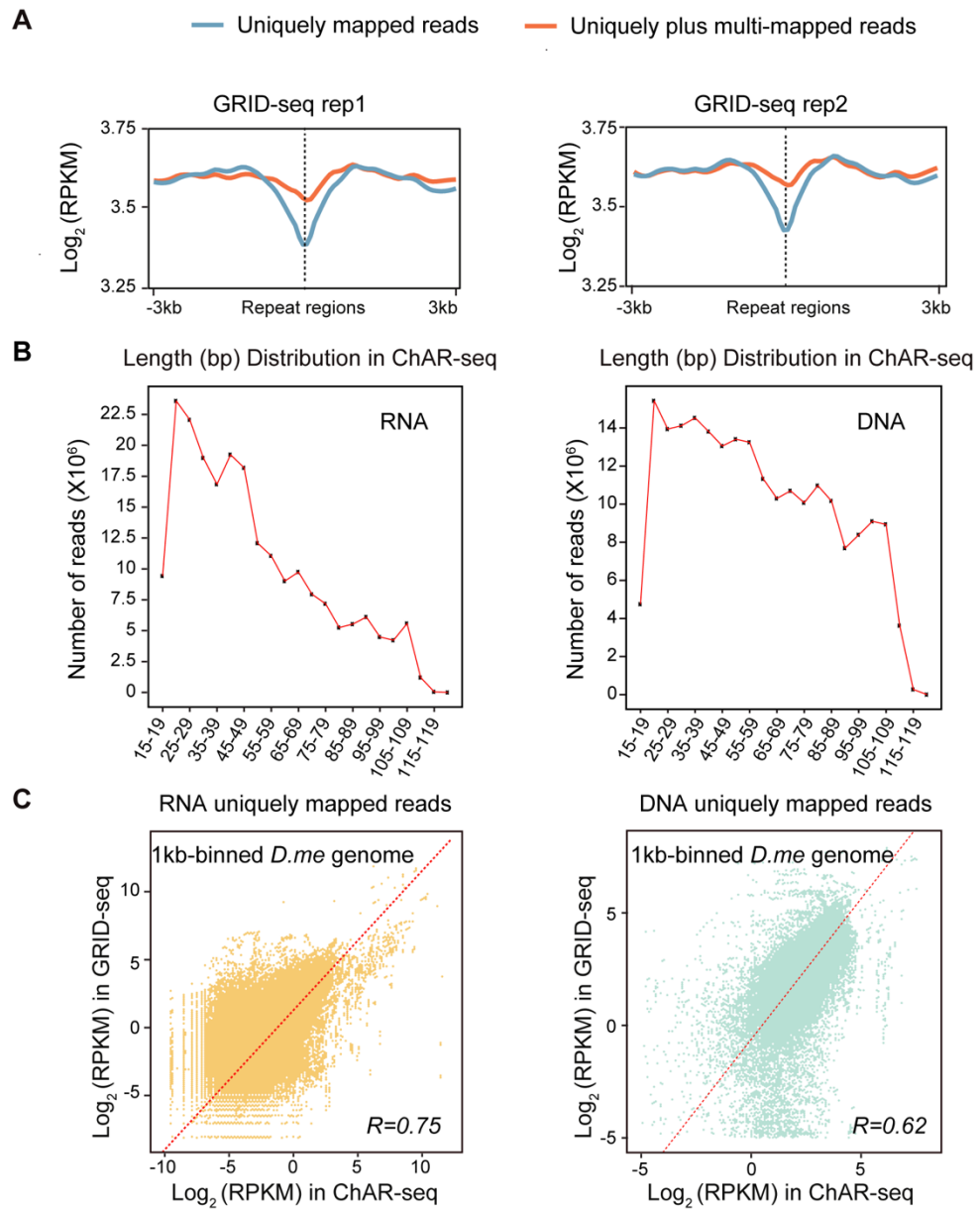
Supplemental_Fig_S1



Supplemental Fig S1. Strategy for assigning multi-mapped RNA and DNA reads

(A) Correlation between DNA (left) or RNA (right) levels in 1 kb-binned *Drosophila* genome between the two independent GRID-seq libraries. RPKM: Reads *per kilobase per million*. (B) Proportions of uniquely mapped, multi-mapped and unmapped RNA or DNA reads identified in the two independent GRID-seq libraries. (C) The ShortStack strategy for assigning multi-mapped reads proportionally to uniquely mapped reads in individual bins. (D) A typical genomic region displaying non-specific RNA binding signals on DNA based on human RNA mapped to the fly genome, raw GRID-seq or ChAR-seq RNA-DNA interaction signals, and background-corrected GRID-seq signals.

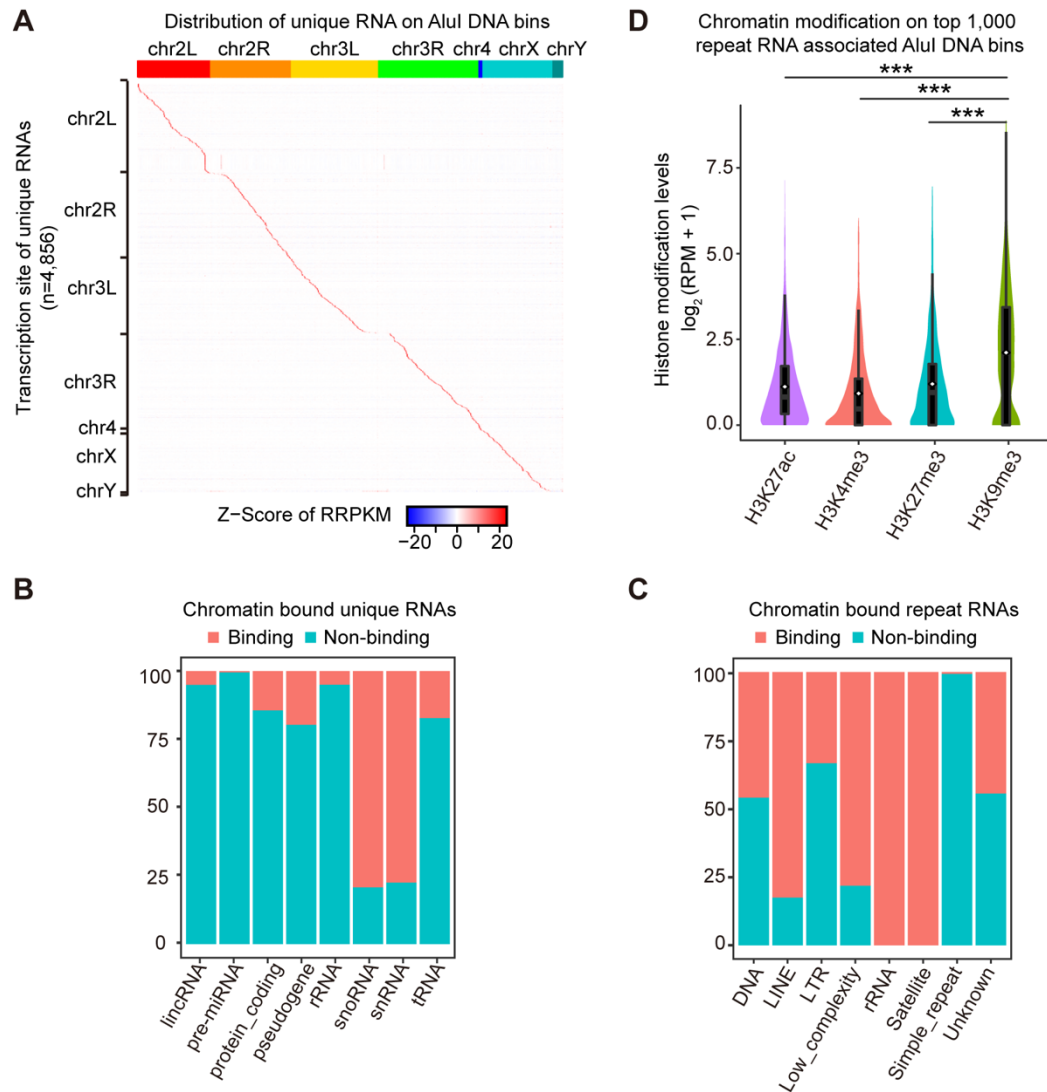
Supplemental_Fig_S2



Supplemental Fig S2. Strategy for assigning multi-mapped RNA and DNA reads

(A) Distribution of RNA interaction signals on the center of repeat-rich DNA regions before and after assigning RNA-DNA interaction reads that contain multi-mapped RNAs. RPKM: Reads *per* kilobase *per* million. (B) The length distribution of RNA (left panel) and DNA (right panel) from the combined ChAR- seq dataset. (C) Comparison between GRID-seq and ChAR-seq libraries using uniquely mapped RNA (left panel) or DNA (right panel) reads in 1kb-binned *Drosophila* genome.

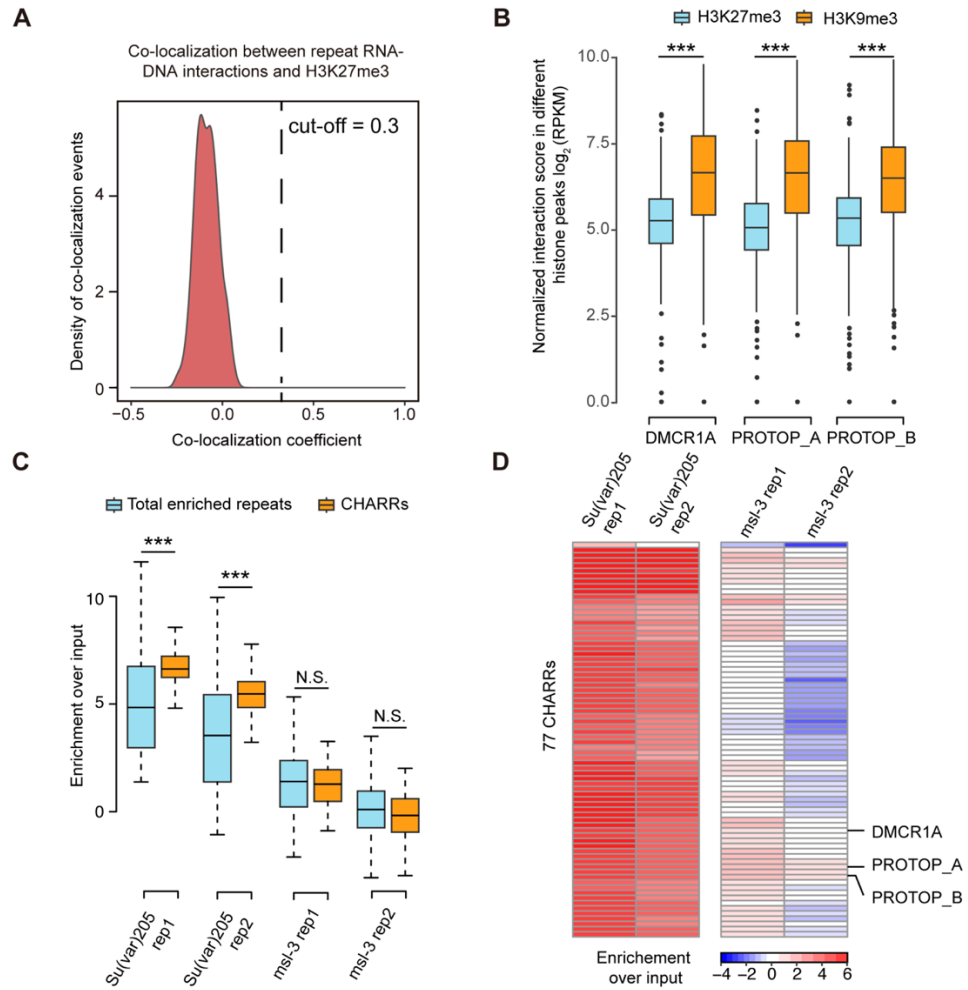
Supplemental_Fig_S3



Supplemental Fig S3. Interaction of different RNA classes with DNA

(A) Heatmap of 4,856 annotated unique RNAs on AluI-generated DNA bins across the *Drosophila* genome in S2 cells. (B) Different unique RNA classes and the percentage of different RNA species in each class involved in interactions with DNA. (C) Different repeat RNA classes and the percentage of different RNA species in each class involved in interactions with DNA. (D) Chromatin modification signals of top 1,000 repeat-derived RNAs on AluI DNA bins. *p<0.05 **p<0.01 *** p<0.001 (Wilcoxon rank sum test).

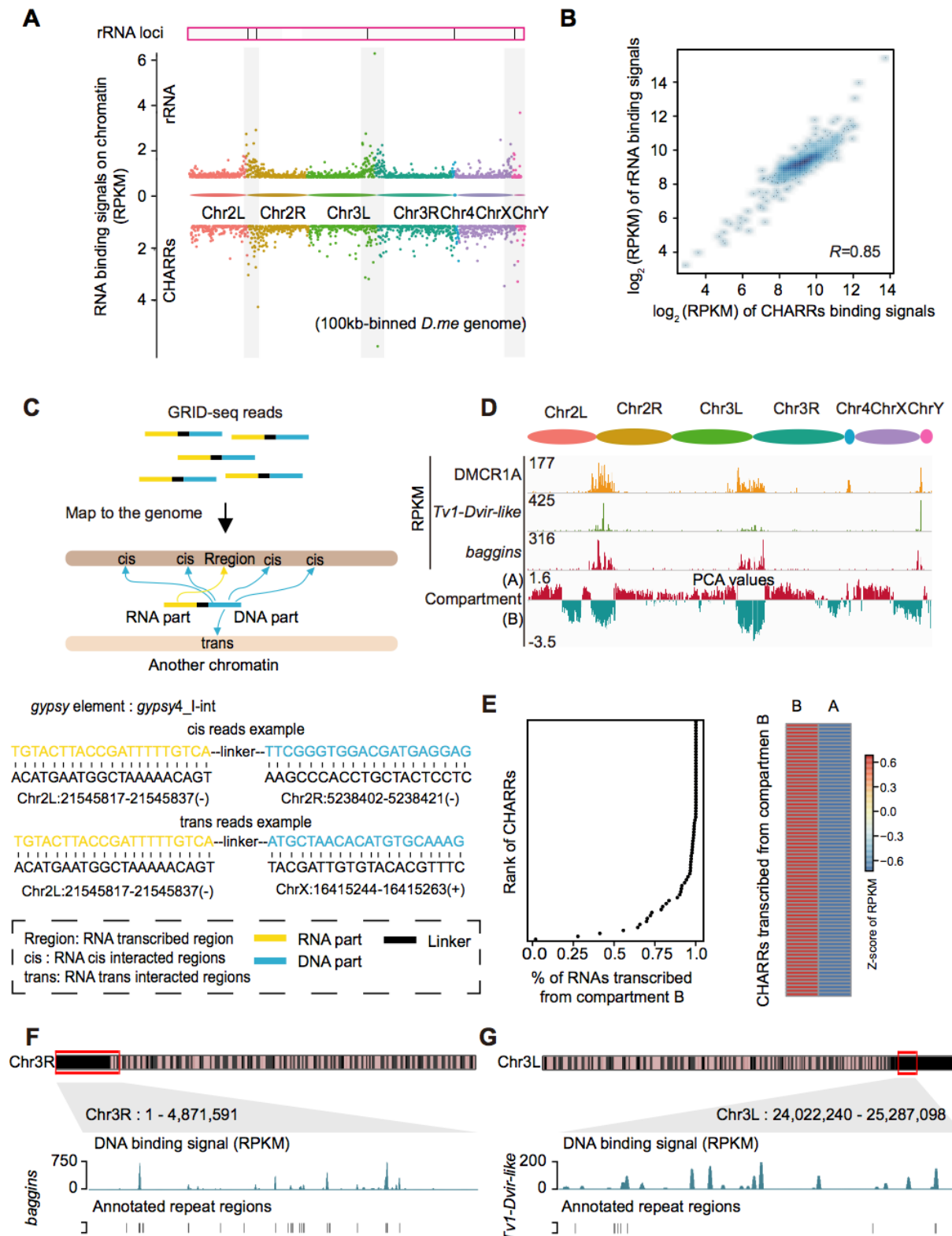
Supplemental_Fig_S4



Supplemental Fig S4. Preferential association of *gypsy*-derived RNAs with constitutive heterochromatin

(A) Distribution of co-localization coefficients between repeat RNA interactions with DNA and the levels of H3K27me3. All co-localization events fall below the set threshold of 0.3 for H3K9me3 and Su(var)205 (see Fig. 3A). (B) The interaction scores of 3 specific CHARRs as indicated on H3K27me3 peaks (blue box) relative to H3K9me3 peaks (orange box). ***p < 0.001 (unpaired Student's t-test). (C) The distribution of \log_2 enrichment scores for total repeat-derived RNAs in comparison with CHARRs (obtained from published paper) from published pulldown experiment with Su(var)205-BioTAP or msl-3-BioTAP complexes in S2 cells. ***p < 0.001 (unpaired Student's t-test). N.S.: not significant. (D) Heatmap showing \log_2 enrichment score of CHARRs in Su(var)205-BioTAP or msl-3-BioTAP pulldown and RNA-seq analysis. Rows: individual CHARRs. Three representative CHARRs illustrated in Fig. 3C are labeled on the right.

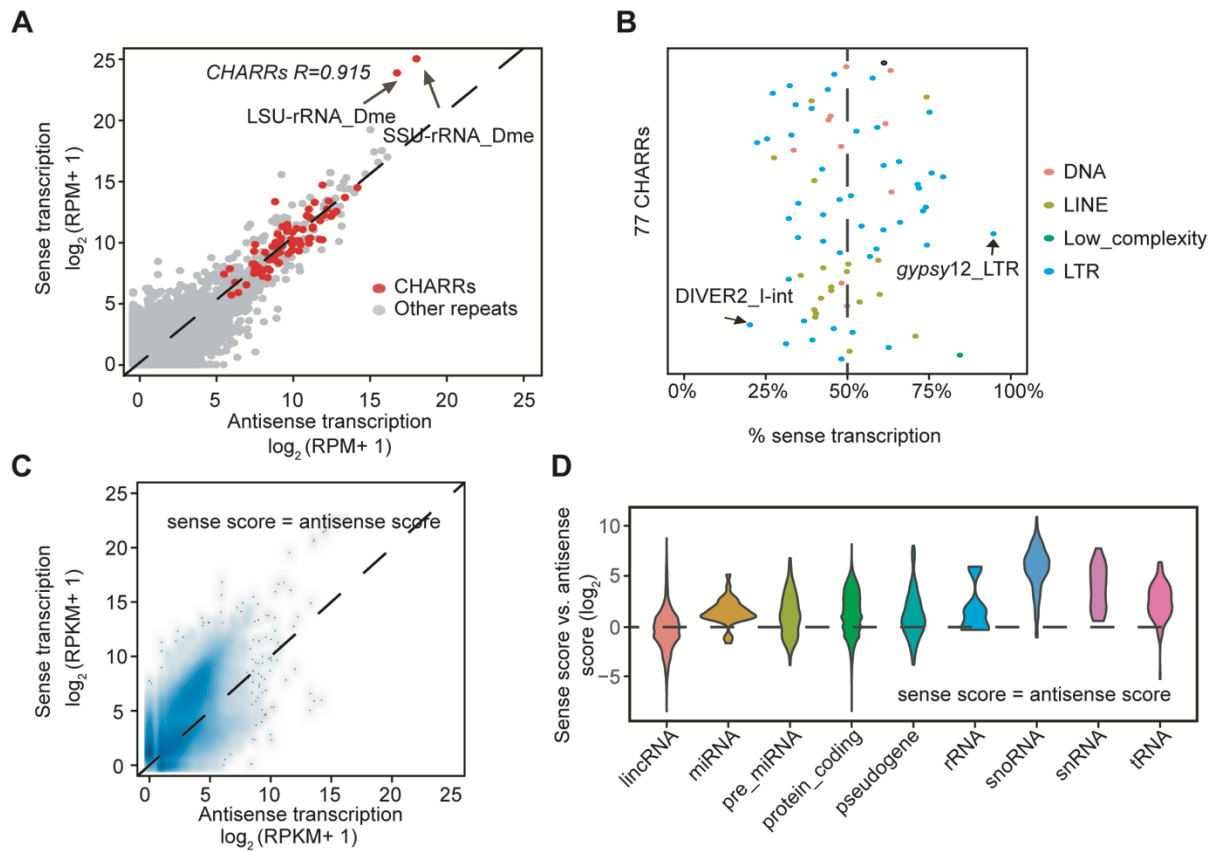
Supplemental_Fig_S5



Supplemental Fig S5. Interactions of rRNAs and CHARRs with DNA

(A) Top: Bars indicate the active rRNA transcription loci in the *Drosophila* genome. DNA binding signals for rRNA and CHARRs in 100 kb windows. Different colors indicate different chromosomes. Grey regions highlight elevated rRNA-DNA interaction regions, which are also associated with enriched binding signals for CHARRs. RPKM: Reads *per* kilobase *per* million. (B) The expression of CHARR binding (*x*-axis) and rRNA (*y*-axis) signals on individual DNA bins. The Spearman correlation coefficient (R) is indicated. RPM: Reads *per* million. (C) Overview on definition of *cis* versus *trans* interactions for individual CHARRs. (D) The interaction score of DMCR1A, *Tv1-Dvir-like*, and *baggins* on Hi-C defined compartment A or B based on positive or negative principal component analysis (PCA) values. RPKM: Reads *per* kilobase *per* million. (E) Rank of CHARRs according to their percentages of RNA transcribed from compartment B (Left panel). Heatmap of normalized interactions scores of compartment B-derived CHARRs in interactions compartment A or B regions (Right panel). (F) *baggins* RNA mostly interacts with DNA with the same repeat sequences, as indicated at bottom track. (G) *Tv1-Dvir-like* RNA interacts with a DNA region mostly lacking the same repeat sequence, as indicated at bottom track.

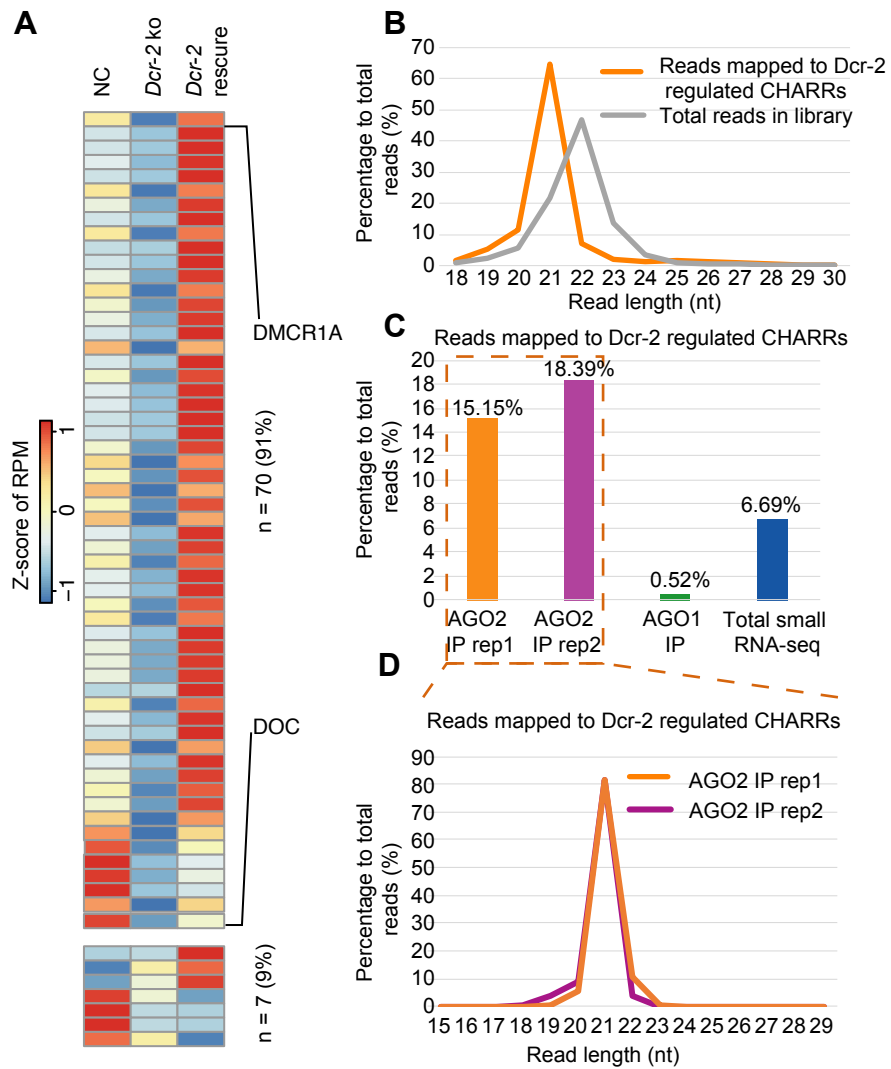
Supplemental_Fig_S6



Supplemental Fig S6. Convergent transcription of repeat RNAs

(A) Scatterplot of sense verse anti-sense transcription of repeat-derived RNAs based on the GRO-seq data from S2 cells. Identified CHARRs are highlighted in red. Arrows point to the two major rRNA transcripts. (B) Percentage of sense transcription-derived RNA for individual CHARRs in S2 cells. Different colors indicate different repeat classes CHARRs are derived from. Two represented CHARRs, DIVER2-I-int and *gypsy12_LTR*, are highlighted. (C) Sense and antisense transcription of annotated unique RNAs. (D) Violin plots showing relative levels of sense and antisense transcription of different classes of non-repeat RNAs.

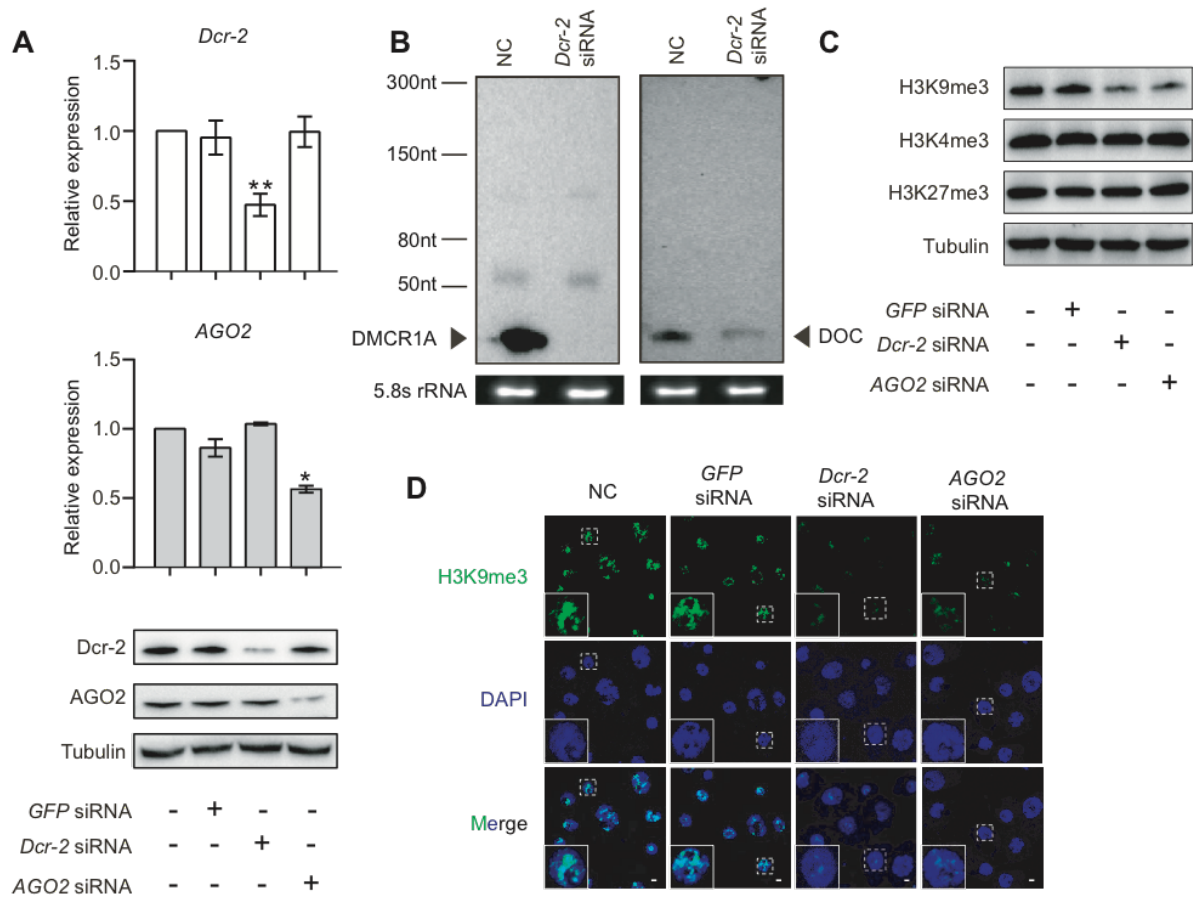
Supplemental_Fig_S7



Supplemental Fig S7. A group of CHARRs show siRNA properties

(A) Heatmap illustrating the expression of CHARRs in response to *Dcr-2* knockout and rescue. Labeled on the left are two representative CHARRs DMCR1A and DOC. ko: knockout. (B) The length distribution of reads mapped to *Dcr-2* regulated CHARRs based on the published small RNA-seq dataset in wild-type female fly heads. (C) The percentage of reads mapped to *Dcr-2* regulated CHARRs over total mapped reads in different small RNA-seq library in S2 cells. (D) The length distribution of reads mapped to *Dcr-2* regulated CHARRs in two different AGO2 IP small RNA-seq libraries.

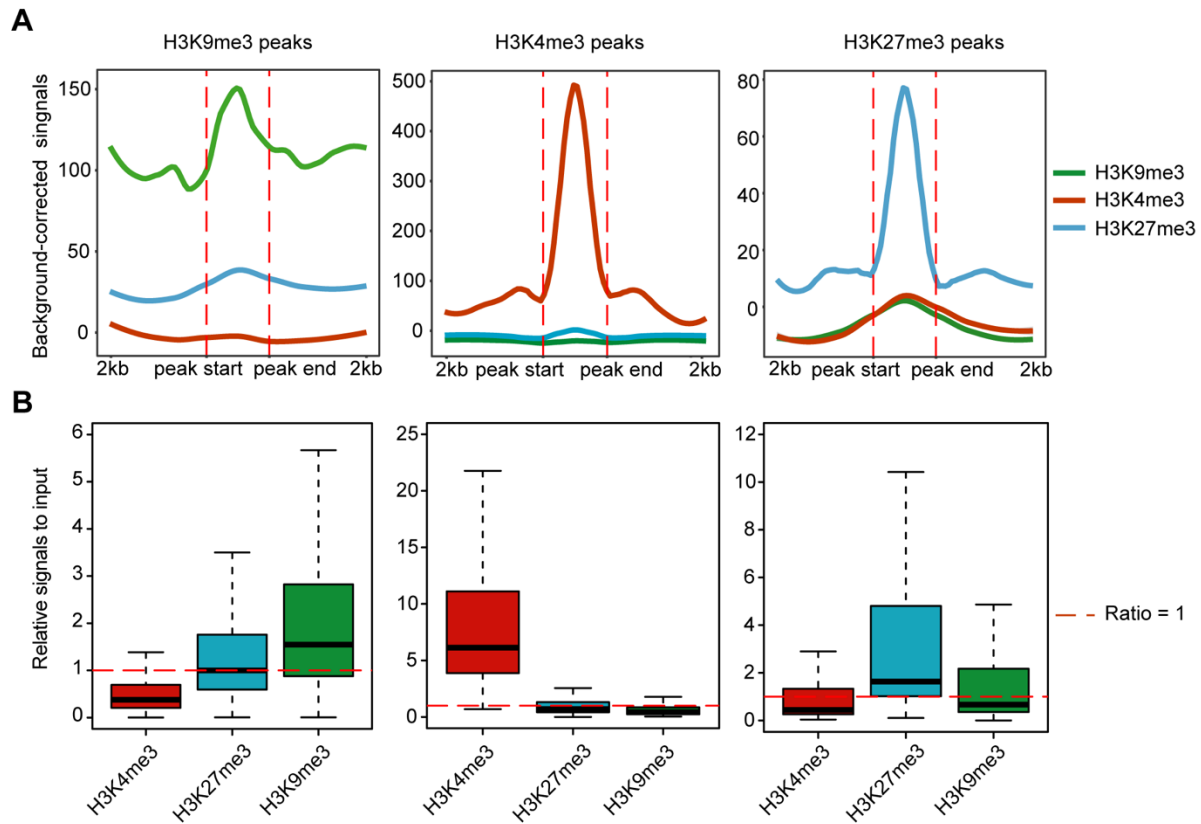
Supplemental_Fig_S8



Supplemental Fig S8. *Dcr-2* mediated processing of repeat RNAs

(A) Confirmation of *Dcr-2* and *AGO2* knockdown in S2 by RT-qPCR and Western blotting analysis. ** $p < 0.01$, * $p < 0.05$ from 3 technical repeats (unpaired Student's *t*-test). (B) Confirmation of *Dcr-2* dependent expression of DMCR1A (left) and DOC (right) expression by Northern blotting analysis. (C and D) The level of H3K9me3, H3K27me3, H3K4me3 and Tubulin in S2 cells in response to siRNA-mediated knockdown of *Dcr-2* and *AGO2* detected by Western blotting analysis (C) and immunocytochemistry (D), Green, H3K9me3 signals; blue, DAPI. Scale bar, 2 μ m.

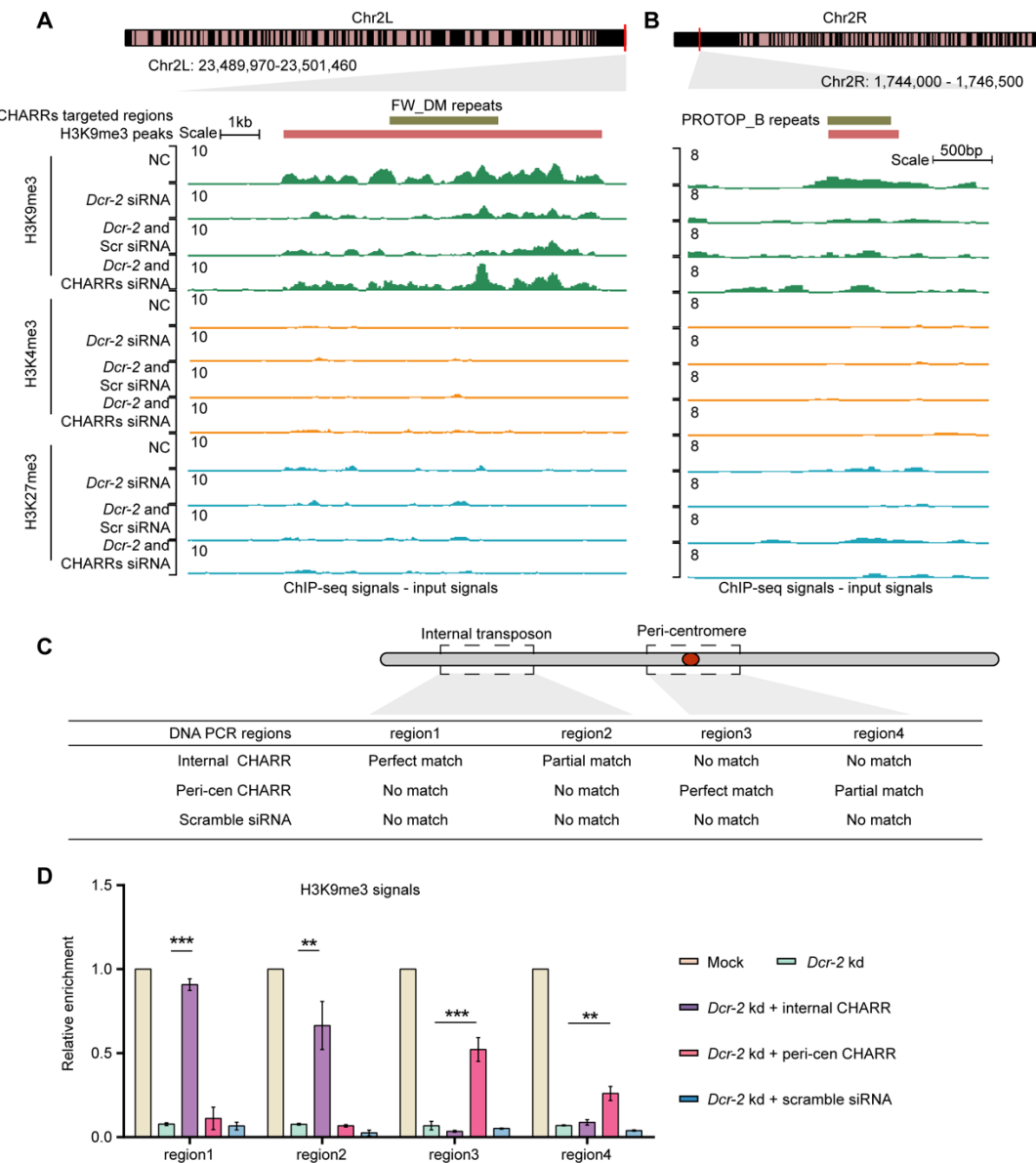
Supplemental_Fig_S9



Supplemental Fig S9. Comparation of the ChIP-seq profiles generated in this study with public data sets

(A) Distribution of indicated histone modification signals around corresponding peaks deduced from the public datasets. (B) Boxplots showing fold changes of histone modification signals on corresponding peaks deduced from the public datasets. Red dash: background ChIP-seq signals.

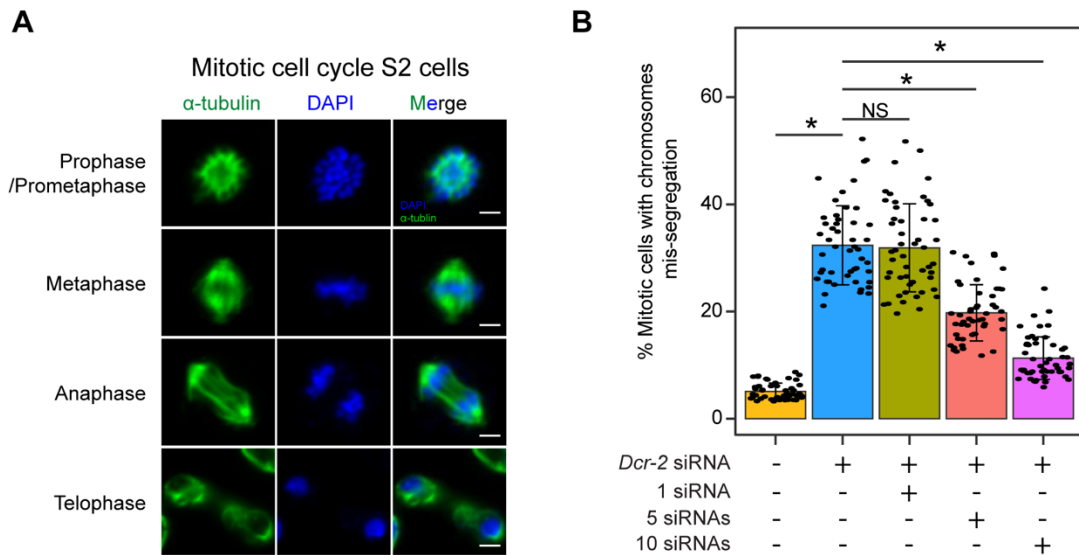
Supplemental_Fig_S10



Supplemental Fig S10. CHARRs-derived siRNAs specifically rescued their target regions

(A and B) A representative a CHARR-targeted (A) or non-CHARR-targeted (B) genomic locus, showing reduced H3K9me3 ChIP-seq signals in response to *Dcr-2* knockdown, complemented with scrambled or CHARRs-derived siRNAs. Signals for H3K4me3 and H3K27me3 were also displayed for comparison. (C) Selection for two internal and two pericentromeric regions for testing the targeting specificity of specific CHARR mimics. (D) ChIP-qPCR analysis of heterochromatin levels in four different regions, two of which are targeted by the internal CHARR mimics and the other two by the pericentromeric (peri-cen) CHARR. Data are presented as mean \pm SEM (n = 3 biological replicates). **p<0.01, ***p<0.001 (Student's *t*-test).

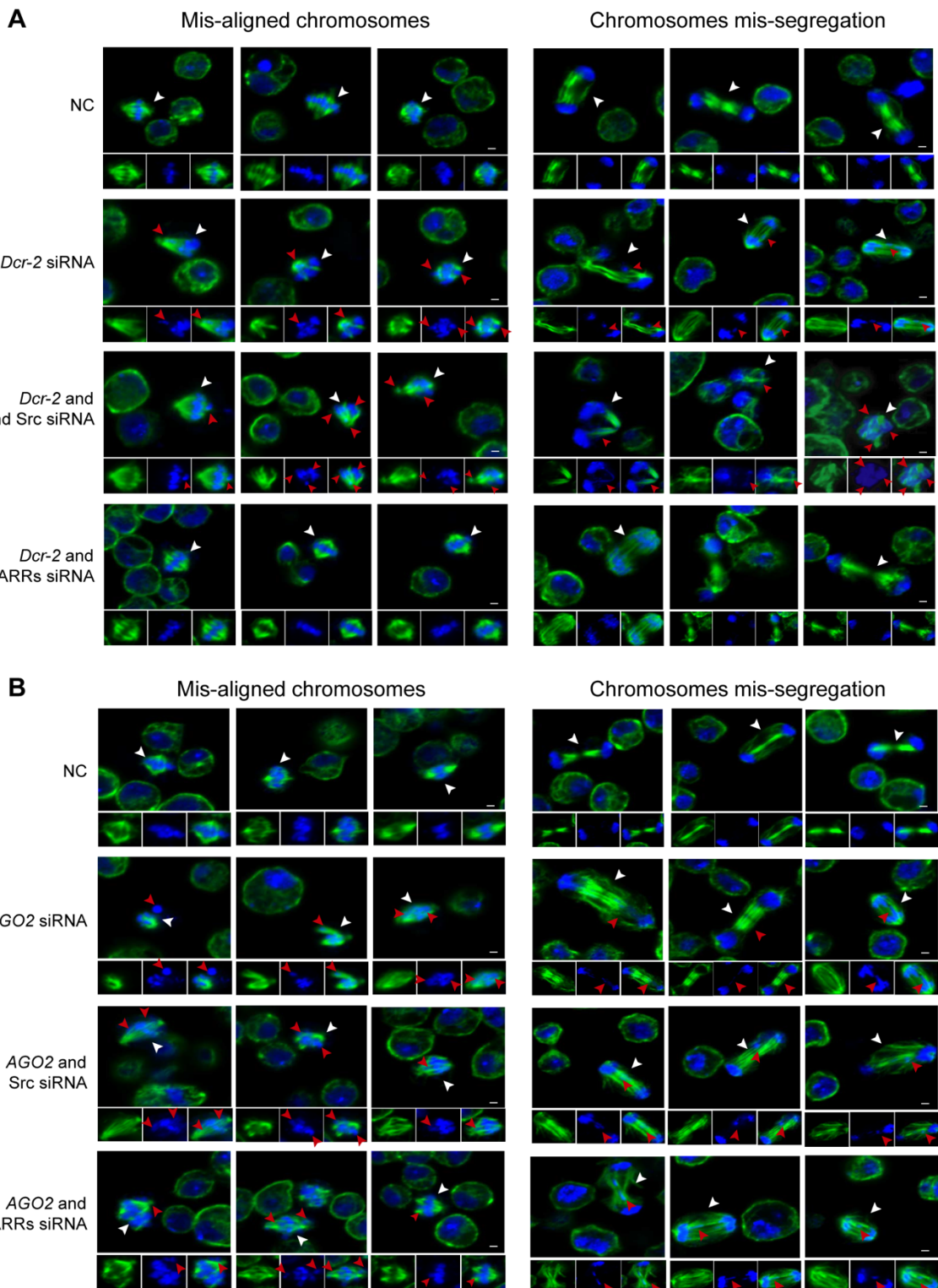
Supplemental_Fig_S11



Supplemental Fig S11. The cell division associated phenotype in S2 cells

(A) Immunostaining of α -tubulin (green) and DAPI-stained DNA (blue) in *Drosophila* S2 cells during cell cycle. Bar, 2 μ m. (B) Percentages of S2 cells at metaphase exhibiting mis-segregation at different experimental conditions. n=50 for each condition. *p<0.05, NS: not significant (multiple group Student's *t*-test).

Supplemental_Fig_S12



Supplemental Fig S12. CHARRs could rescue *Dcr-2* knockdown, but not *AGO2* knockdown-induced cell division defects

(A) Examples of typical chromosomes mis-alignment (left) or mis-segregation (right) phenotype in response to *Dcr-2* knockdown and after treatment with scrambled or CHARRs-derived siRNAs. Green: α -tubulin; Blue: DAPI-stained DNA. White arrows indicate abnormal cells; Red arrows indicate abnormal loci in specific cells. Scale bars: 2 μ m. (B) Similar analysis as in A, except in *AGO2* knockdown cells.

Supplemental Table S1. Statistics of GRID-seq and ChAR-seq data

Library Name	Useful Reads Number	Unique RNA-DNA pairs	Multiple RNA-unique DNA pairs	Unique RNA -multiple DNA pairs	Multiple RNA-DNA pairs
GRID-seq rep1	95.7M	20.9M	32.1M	5.9M	10.3M
GRID-seq rep2	74.0M	5.8M	8.9M	1.3M	2.7M
ChAR-seq rep1	6.7M	1.8M	1.4M	0.4M	0.3M
ChAR-seq rep2	14.8M	4.5M	4.1M	0.9M	0.8M
ChAR-seq rep3	7.2M	0M	0M	0M	3.5M
ChAR-seq rep4	2.5M	0.6M	0.6M	0.1M	0.1M
ChAR-seq rep5	186.7M	58.8M	54.8M	13.9M	12.1M

Supplemental Table S2. Sequencing datasets used in this study

Data type	Cell type	Accession ID
GRO-seq	<i>Drosophila</i> S2	GSM577244
H3K4me3 ChIP-seq	<i>Drosophila</i> Embryos 20-24h	GSM400672
H3K9me3 ChIP-seq	<i>Drosophila</i> Embryos 20-24h	GSM439452
H3K27me3 ChIP-seq	<i>Drosophila</i> Embryos 20-24h	GSM439443
H3K27ac ChIP-seq	<i>Drosophila</i> Embryos 20-24h	GSM401423
Input ChIP-seq (H3K4me3, H3K9me3, H3K27me3, H3K27ac)	<i>Drosophila</i> Embryos 20-24h	GSM400673
Pol II5S ChIP-Seq	<i>Drosophila</i> S2	GSM577243
Su(var)205 ChIP-seq	<i>Drosophila</i> S2	GSM628252
Su(var)205 input ChIP-seq	<i>Drosophila</i> S2	GSM628253
Hi-C	<i>Drosophila</i> S2	GSM1420136
AGO2 IP small RNA-seq rep1	<i>Drosophila</i> S2	GSM280087
AGO2 IP small RNA-seq rep2	<i>Drosophila</i> S2	GSM266765
AGO1 IP small RNA-seq	<i>Drosophila</i> S2	GSM280088
Small RNA-seq in S2 cells	<i>Drosophila</i> S2	GSM272652
small RNA-seq in the control flies	Female fly heads	GSM2241581
small RNA-seq in the <i>Dcr-2</i> [null] flies	Female fly heads	GSM2241582
small RNA-seq in the <i>Dcr-2</i> [null] rescued by the transgenic <i>Dcr-2</i>	Female fly heads	GSM2241583
ChAR-seq rep1	CME-W1-cl8+ wing-disc cell line	GSM2552075
ChAR-seq rep2	CME-W1-cl8+ wing-disc cell line	GSM2552076
ChAR-seq rep3	CME-W1-cl8+ wing-disc cell line	GSM2552077
ChAR-seq rep4	CME-W1-cl8+ wing-disc cell line	GSM2552078
ChAR-seq rep5	CME-W1-cl8+ wing-disc cell line	GSM2552079

Supplemental Table S3. List of primer sequences and siRNAs used in this study

Primer /siRNAs	Sequence (5' to 3')	Assay
<i>Dcr-2</i> Primer (forward)	TACGCCCTGAGCTGCGAAACG	qRT-PCR
<i>Dcr-2</i> Primer (reverse)	GTCCCGAAACTGCTGAATGG	qRT-PCR
<i>AGO2</i> Primer (forward)	TTCACCCTGCCACAACAA	qRT-PCR
<i>AGO2</i> Primer (reverse)	CCTCGTATCCATCATCCAGTTC	qRT-PCR
Gapdh Primer (forward)	ACCTATGACGAAATCAAGGCTAA	qRT-PCR
Gapdh Primer (reverse)	GCTGAAGAAGTCGGTGGAGA	qRT-PCR
dsRNA ^a <i>GFP</i> siRNA (forward)	TAATACGACTCACTATAGGGATGGTGAGC AAGGGCGAG	<i>GFP</i> knockdown
dsRNA ^a <i>GFP</i> siRNA (reverse)	TAATACGACTCACTATAGGGTTACTTGTA CAGCTCGTCCATGCC	<i>GFP</i> knockdown
dsRNA ^a <i>Dcr-2</i> siRNA (forward)	TAATACGACTCACTATAGGGAGAATCGGC TATCACCTTGTGG	<i>Dcr-2</i> knockdown
dsRNA ^a <i>Dcr-2</i> siRNA (reverse)	TAATACGACTCACTATAGGGAGAATTCCC AAAACGCTAACAC	<i>Dcr-2</i> knockdown
dsRNA ^a <i>AGO2</i> siRNA (forward)	TAATACGACTCACTATAGGGTTATATGAA TGACCGAATTTCGAC	<i>AGO2</i> knockdown
dsRNA ^a <i>AGO2</i> siRNA (reverse)	TAATACGACTCACTATAGGGTTAGGGC CTGACCTTCCTCGATG	<i>AGO2</i> knockdown
DMCR1A ^b	CUAACCGUAGAACUAUGCUUG	CHARRs mix
FB4_DM ^b (rep1)	UUUAAGAGUGGGCAAACGAAA	CHARRs mix

FB4_DM^b (rep2)	CGUUUGCCCACUCUUAAAACU	CHARRs mix
<i>gypsy4_I-int^b (rep1)</i>	AUGAAUUCUGUAGACUCCUUU	CHARRs mix
<i>gypsy4_I-int^b (rep2)</i>	AUAGGAACCCAAAUGCGAAG	CHARRs mix
FW_DM^b (rep1)	CUUGUUGAACAGCAUACCACU	CHARRs mix
FW_DM^b (rep2)	UUACACUAGCGGCCGUAUACU	CHARRs mix
DOC^b	UAAAAAUAAUCAAGCUGUUGC	CHARRs mix
<i>gypsy2-I_DM^b</i>	AAAAUACGAAUUUCGCAGACU	CHARRs mix
I_DM^b	UUGCCCAGGCCUCUGAUGAUU	CHARRs mix
DOC	TAATACGACTCACTATAGGGAGAATAAAA TAATCAAGCTGTTGC	Northern blot
DMCR1A	TAATACGACTCACTATAGGGAGAACTAAC CGTAGAACTATGCTTG	Northern blot
<i>gypsy4_I-int</i>	TAATACGACTCACTATAGGGCTTCGCATT TGGGTTCCCTAT	Northern blot
<i>gypsy2-I_DM</i>	TAATACGACTCACTATAGGGAGTCTGCGA AATTCTGTATTT	Northern blot
Region1 Primer (forward)	CGGCTCCAAAGCGAATGT	ChIP-qPCR
Region1 Primer (reverse)	GCGACAAGCAACGTGAGTAT	ChIP-qPCR
Region2 Primer (forward)	ACCCATTAGTCTGCCATCATTAG	ChIP-qPCR
Region2 Primer (reverse)	GCTAGGCCTTCGTCGATT	ChIP-qPCR
Region3 Primer (forward)	CATTTTAACGTTGCCACCCCTT	ChIP-qPCR

Region3 Primer (reverse)	TTTAGTTTAAAAGGTGGGCAATCG	ChIP-qPCR
Region4 Primer (forward)	CAGCATAACATACAAACATGAGTAAC TG	ChIP-qPCR
Region4 Primer (reverse)	GCCCACAAATTGCCACACT	ChIP-qPCR
Internal CHARR^b	UAACGAAAUGAUUUCUUAC	ChIP-qPCR
Peri-cen CHARR^b	CGUUUGCCCACUCUUAAAACU	ChIP-qPCR
Scramble siRNA^b	UUGUACUACACAAAAGUACUG	ChIP-qPCR/rescue experiments

^aDouble strand RNAs

^bendo-siRNA mimics

Supplemental Table S4. List of plasmids, antibodies and assay kits used in this study.

Plasmids/Antibodies /Assay kits	Source	Identifier
pEGFP-N1	Addgene	6085-1
Rabbit monoclonal anti-Dcr-2	Abcam	Cat#ab4732; RRID: AB_449344
Rabbit monoclonal anti-H3K9me3	Abcam	Cat#ab8898; RRID: AB_306848
Rabbit monoclonal anti-H3K27me3	Millipore	Cat#07-449; RRID: AB_310624
Rabbit monoclonal anti-H3K4me3	Millipore	Cat#04-614; RRID: AB_1587134
Mouse monoclonal anti-Tubulin	Abcam	Cat#ab44928; RRID: AB_2241150
T7 RNA polymerase	Promega	P2075
ULYSIS Nucleic Acid Labeling Kit	Thermo Fisher Scientific	U21654
Biotin RNA labeling mix	Roche	11685597910
Chemiluminescent Nucleic Acid Detection Module	Thermo Fisher	89880
NucleoSpin RNA Clean-up XS	MN	740903.50
NorthernMax kit	Thermo Fisher	AM1940
Formaldehyde	Sigma-Aldrich	252549-100ML
Protein A/G Magnetic Beads	Thermo Fisher	88803
Protease Inhibitor	MCE	HY-K0010
Proteinase K	Ambion	25530015
Phenol:chloroform:Isoamyl	Sigma	P2069
TransScript II Green One-Step qRTPCR SuperMix	Transgene	AQ311-02
DAPI	Thermo Fisher	R37605
Goat anti-Mouse IgG Secondary Antibody, Alexa Fluor 488	Invitrogen	A-11029